Journal of Herpetology, Vol. 0, No. 0, 000–000, year

Phylogeography of the Rough Greensnake, *Opheodrys aestivus* (Squamata: Colubridae), Using Multilocus Sanger Sequence and Genomic ddRADseq data

Eric N. Rittmeyer,[1] Ahmed Elmonier,[1] and Sara Ruane[1,2]

[1]*Department of Biological Sciences, Rutgers University – Newark, 195 University Ave, Newark, New Jersey, USA 07102*

Abstract.—**The Rough Greensnake, *Opheodrys aestivus*, is a moderately sized, semi-arboreal snake broadly distributed throughout eastern North America. Although numerous taxa with similar distributions have been shown to comprise multiple species, *O. aestivus* has not been examined in a detailed phylogeographic context. Here, we use Sanger-sequence data (one mitochondrial, three nuclear loci) for samples from throughout the distribution of *O. aestivus* to elucidate phylogeographic patterns in this species. We combine this with ddRADseq data for a subset of samples to test patterns on a more genomically comprehensive scale. In both data sets, we find strong support for three deeply divergent clades within *O. aestivus*: peninsular Florida, central Texas, and a Main clade comprising the rest of the distribution. Estimates of divergence time suggest that the central Texas and Main clades diverged ~1.3 million years ago (mya), while the peninsular Florida clade diverged from other lineages ~2.9 mya, and these lineages diverged from the sister taxon, *O. vernalis*, ~6.4 mya. The divergence of peninsular Florida or central Texas populations is not unique among squamates, nor is low levels of divergence from the Atlantic coast to eastern Texas, but this combination of patterns is unusual and yields important insight into the biogeography of North American biota. Further, our approach helps illustrate how dense geographic sampling with limited genomic sequencing can be used as a guide for the selection of samples to test phylogeographic patterns comprehensively. We conclude that elevating *O. a. carinatus* to species status may better describe the diversity of this genus.**

Assessing phylogeographic structure within species is a critical aspect for making robust, fine-scale inferences regarding the evolutionary history of populations and taxa (Avise, 2000; Hickerson et al., 2010; Riddle, 2016; Rissler, 2016; Kumar and Kumar, 2018). Failure to account for such structure can bias downstream analyses and inferences, and may also impede conservation efforts (Coyne and Orr, 2004; Isaac et al., 2004; Bickford et al., 2007; Edwards et al., 2007; Bortolus, 2008; Hickerson et al., 2010; Kajtoch et al., 2016; Médail and Baumel, 2018; Jackson and Cook, 2020). Treating multiple distinct populations as a single entity can result in inflated estimates of genetic diversity and population size estimates, while oversplitting single lineages may have the opposite result. Understanding the phylogeographic patterns within taxa can also further help elucidate how species may have responded to historic climatic fluctuations (e.g., Pleistocene glacial cycles), and thus help to predict how taxa may respond to future climate change (Provan and Bennett, 2008; Row et al., 2011; D'Amen et al., 2013; DiLeo et al., 2013; Papadopoulou and Knowles, 2016; Mascarenhas et al., 2019; Nadeau and Urban, 2019; Luna-Aranguré and Vázquez-Domínguez, 2020).

North America is an intriguing region for phylogeographic inference because many taxa are broadly distributed across the continent, and recent glaciations during the Pleistocene have likely restricted species to refugia in the southern portions of their current ranges (Swenson and Howard, 2005; Waltari et al., 2007; Provan and Bennett, 2008; Polfus et al., 2017; Lait and Hebert, 2018). Further, multiple geographic features have been shown to be important barriers to gene flow among populations, including the Mississippi and Apalachicola rivers. Indeed, several taxa previously thought to represent single, broadly distributed taxa in this region have, upon more comprehensive (often molecular) investigation, been shown instead to be multiple distinct and geographically segregated species (Burbrink et al., 2000; Burbrink, 2001; Leaché and Reeder, 2002; Lemmon et al., 2007; Crother et al., 2011; Ruane et al., 2014; Barrowclough et al., 2019; Guyer et al., 2020; Jackson and Cook, 2020).

Among these taxa widely distributed across eastern North America is the Rough Greensnake, *Opheodrys aestivus*, a moderately sized (maximum snout–vent length = 735 mm; Walley and Plummer, 2000) semi-arboreal species with a broad distribution throughout much of eastern North America, ranging from the Pine Barrens of southern New Jersey in the northeast, south to the Florida Keys, and west to northeastern Mexico and the Edwards Plateau of central Texas (Walley and Plummer, 2000; Powell et al., 2016). In the most comprehensive taxonomic review of the species, Grobman (1984) used scalation data from throughout the range and recognized four subspecies: *O. a. carinatus* from peninsular Florida, *O. a. conanti* from Virginia barrier islands, *O. a. majalis* from the western portion of the range (primarily Texas, Oklahoma, western Arkansas, Missouri, and Kansas), and *O. a. aestivus* from the rest of the distribution. Subsequent authors, however, have recognized only *O. a. aestivus* and *O. a. carinatus*, arguing that *O. a. conanti*, *O. a. majalis*, and *O. a. aestivus* represent the arbitrarily divided portions of clinal variation across the range of the species (Frost and Hillis, 1990; Frost et al., 1992; Walley and Plummer, 2000). Whether any of these subspecies represent distinct, evolutionary lineages has yet to be tested.

Here, we use multilocus Sanger-sequence data from samples throughout the distribution of *O. aestivus* to examine phylogeographic structure and infer the timing of divergence among lineages, while simultaneously determining whether any of the historically recognized subspecies are in fact supported as distinct lineages of *Opheodrys*. We supplement Sanger-sequence data with genomic data collected via double-digest restriction associated DNA sequencing (ddRADseq) for a subset of samples spanning the distribution and all major clades recovered in the Sanger data set to provide a more genomically comprehensive test of the lineages and putative species boundaries.

[2]Corresponding author. E-mail: sara.ruane@rutgers.edu
DOI: 10.1670/20-040

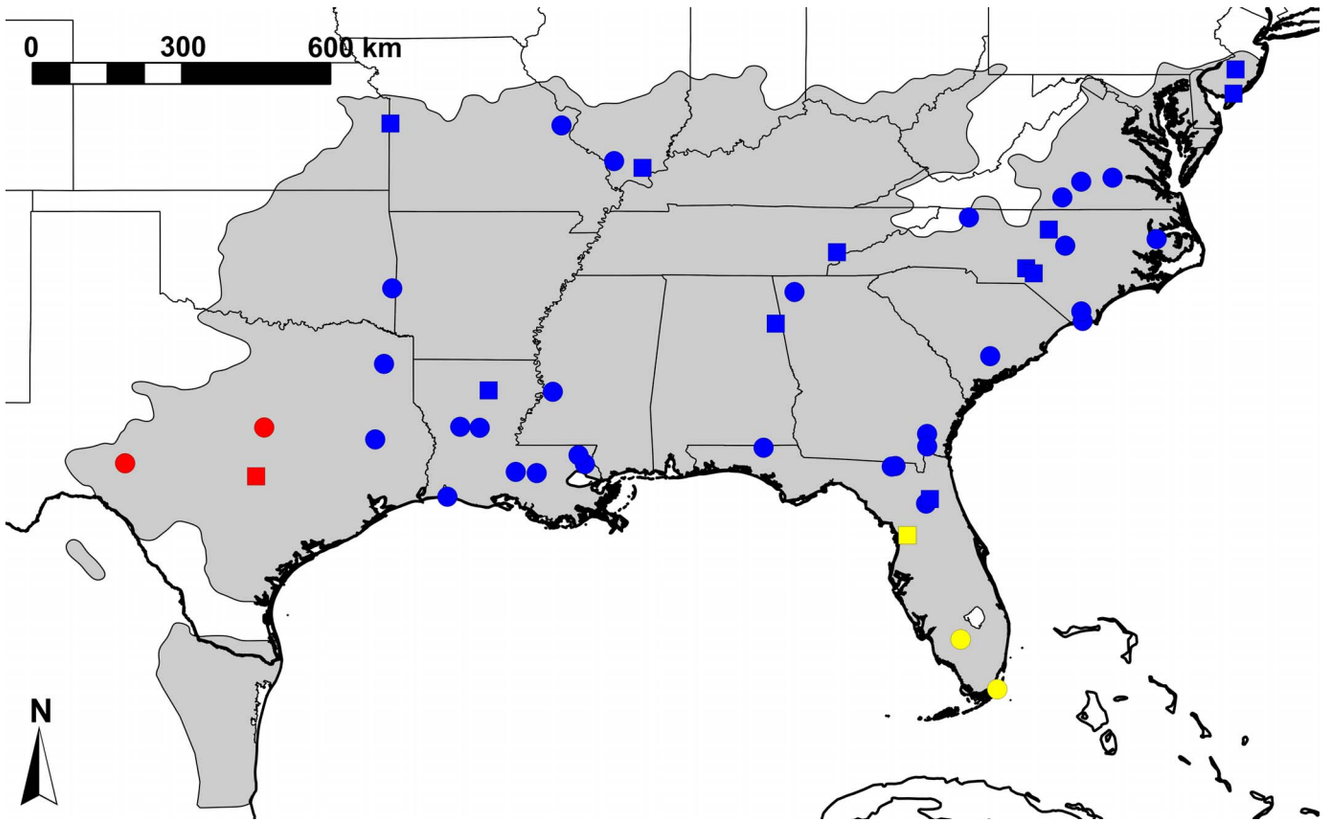

FIG. 1. Sampling localities for *Opheodrys aestivus* included in this study, with the distribution of the species based on IUCN Red List data (Hammerson et al., 2007) shown in grey. Symbol color corresponds to clade: yellow: peninsular Florida clade, red: central Texas clade, blue: Main clade. Squares indicate samples included in both Sanger and ddRADseq datasets, circles indicate samples included only in Sanger data sets.

MATERIALS AND METHODS

Sampling.—We obtained 47 samples of *O. aestivus* from throughout the distribution of the species (Fig. 1), 4 samples from the sister taxon *O. vernalis*, and 1 sample from each of the more distantly related colubrid species *Cemophora coccinea*, *Lampropeltis getula*, *Pantherophis guttatus*, *Pituophis melanoleucus*, and the natricid *Nerodia sipedon* (Appendix). Whole genomic DNA was extracted for all samples using a Qiagen DNeasy Blood and Tissue kit and quantified using a Qubit 2.0 fluorometer with the High Sensitivity kit (Invitrogen, Inc.).

Sanger Sequencing.—For all samples, we targeted one mitochondrial (cytochrome b, cytb) and three nuclear loci (LAT clone, LAT; neurotrophin 3, NT3; and prolactin receptor, PRLR) using the primers and annealing temperatures provided in Table 1. Target loci were amplified via polymerase chain reaction conditions as in Ruane et al. (2014), purified using ExoSAP-IT (ThermoFisher Scientific, Inc.), and sequenced in both directions using amplification primers by Macrogen, USA (Brooklyn, New York, USA). Complementary sequences were then assembled in Geneious ver. 6.1.8 (https://www.geneious.com; Kearse et al., 2012), and sequences were aligned using Muscle (Edgar, 2004). Alignments were visually inspected to check for errors, and protein coding genes were translated to amino acid sequences in Geneious to check for premature stop codons. We used PHASE ver. 2.1.1 (Stephens et al., 2001; Stephens and Scheet, 2005) to estimate the most probable pair of alleles for nuclear sequences with multiple heterozygous sites. For each locus, PHASE analyses were run for 1,000 iterations, sampling every iteration, following 200 iterations of burn-in. We replicated PHASE analyses for each locus three times to ensure results were consistent, using a different random starting seed for each run.

Sanger-Data Phylogeography.—We used maximum likelihood (ML) and Bayesian inference methods to infer the phylogenetic

TABLE 1. Primer and amplification details for loci used in Sanger data set.

Locus	Primer	Sequence	Length (bp)	Annealing temp. (°C)	Reference
Cytb	Cytb-F	GACCTGTGATMTGAAAACCAYCGTTGT	1117	50	(Burbrink et al., 2000)
	Cytb-R	CTTTGGTTTACAAGAACAATGCTTTA			
LAT	CL-LAT-F	CCAGTGTGCTGGAATTCAG	795	47	(Ruane et al., 2014)
	CL-LAT-R	TATCTGCAGCATTCAGGA			
NT3	NT3-F3	ATATTTCTGGCTTTTCTCTGTGGC	519	50	(Noonan and Chippindale, 2006)
	NT3-R4	GCGTTTCATAAAAATATTGTTTGACCGG			
PRLR	PRLR-F1	GACARYGARGACCAGCAACTRATGCC	577	55	(Townsend et al., 2008)
	PRLR-R3	GACYTTGTGRACTTCYACRTAATCCAT			

relationships among populations of *O. aestivus*. Analyses were conducted on (a) each phased locus individually, with the mitochondrial data partitioned by codon position, (b) the three unphased nuclear loci concatenated and partitioned by locus, and (c) a concatenated analysis of mitochondrial and unphased nuclear data, partitioned by mitochondrial codon position and nuclear locus. We estimated the best fit model of nucleotide substitution for each partition in jModeltest 2.0 (Posada, 2008) using the corrected Akaike information criterion (cAIC). We then used RAxML ver. 8.2.12 (Stamatakis, 2007) to estimate the ML phylogenies, with 25 search replicates to find the ML phylogeny using the GTR+G model for each partition, because RAxML only implements the GTR model of nucleotide substitution. Other parameters were left as default values. To estimate branch support for each ML analysis, nonparametric bootstrap analysis based on 1,000 pseudoreplicates was conducted in RAxML. Bayesian phylogenetic analyses were conducted in Mr.Bayes ver. 3.2.7a (Huelsenbeck and Ronquist, 2001; Ronquist and Huelsenbeck, 2003; Ronquist et al., 2012) using the best-fit models of nucleotide substitution for each partition. Two independent runs of 12 million iterations were conducted, sampling every 1,000 iterations, the first 2,000 samples of which were discarded as burn-in. Parameter trends and effective sample sizes (ESSs) were examined in Tracer ver. 1.6 (Rambaut and Drummond, 2007) to ensure runs had converged at stationarity, and the posterior had been sufficiently sampled.

We examined population structure and identified putative lineages within the genus *Opheodrys* for use in multispecies coalescent analyses in Structure ver. 2.3.2 (Pritchard et al., 2000; Falush et al., 2003). Structure analyses were run assuming the possibility of admixture among populations; 20 replicates were run for each value of *K*, with each run consisting of a burn-in of 50,000 iterations, followed by 100,000 iterations of sampling with a thinning interval of 10. The optimal value of *K* was then determined by examining the Ln P(D) plot, and by calculating ΔK (Evanno et al., 2005) using the web interface of CLUMPAK (Kopelman et al., 2015) and Structure Harvester (Earl and VonHoldt, 2012). Clusters identified in initial analyses were then re-analyzed individually because Structure may detect only higher levels of population structure and fail to detect finer scale populations (Evanno et al., 2005).

Species Tree and Divergence Time Estimation.—We used *BEAST v. 2.6.0 to estimate the multispecies coalescent phylogeny for lineages with strong support as distinct lineages in concatenated analyses, as well as to estimate the timing of divergence among these lineages and between the two species of *Opheodrys* (Heled and Drummond, 2010; Bouckaert et al., 2014). Mitochondrial data were partitioned by codon position for model of nucleotide substitution and clock model; but, constrained to a single gene genealogy, nuclear loci were unlinked across substitution model, clock model, and gene genealogies. All partitions were set to an uncorrelated log-normal relaxed clock model, and to nucleotide substitution models following the best-fit model as estimated in jModeltest. Analyses were run for 250 million generations, sampling every 10,000 generations, the first 10% of which were discarded as burn-in. Convergence was determined by examining all parameter plots and ESSs in Tracer. Priors on fossil calibration points were placed on nodes in the species tree because the fossil record reflects the history of species rather than that of allelic lineages, and divergences in any gene genealogies or a concatenated phylogeny necessarily predate divergences in the species tree, thus resulting in an overestimate of divergence time (McCormack et al., 2011). Fossil calibrations were given log-normal prior distributions with mean ages and soft 95% prior distribution boundaries following Pyron and Burbrink (2009a) and based on information in Holman (2000) and Head et al. (2016). We used two fossil records to calibrate the phylogeny of *Opheodrys*: (1) the divergence between *Pantherophis guttatus* and *Pituophis melanoleucus* was given a mean of 16 million years (mya) with a prior credibility interval of 11.9–21.0 mya based on the oldest known fossil *Pantherophis* (Head et al., 2016; Tucker et al., 2014), and (2) the divergence between *Cemophora coccinea* and *Lampropeltis getula* was given a mean of 13.75 mya with a prior credibility interval of 8.4–21.3 mya based on the oldest known kingsnake, *Lampropeltis similis*, from the medial Barstovian age, Miocene epoch.

Demographic Analyses.—To examine the demographic history of *O. aestivus*, and specifically to test the importance of migration among resulting lineages, we used IMa3 (Hey and Nielsen, 2004, 2007; Hey, 2010; Hey et al., 2018) to fit isolation with migration models to the Sanger sequence data. Complexity of the model and difficulties achieving suitable mixing when including all *Opheodrys* samples dictated that IMa3 analyses were restricted to *O. aestivus*, with all *O. vernalis* samples excluded. We tested the fit of five possible demographic scenarios that vary in their history of migration among resulting lineages (see Results below for details on the included lineages: "Main," "Texas," and "Florida"): (1) no migration, (2) migration restricted to between the Main and Texas lineages (i.e., no migration between Florida and other populations, currently or historically), (3) migration only between sister lineages (i.e., between Main and Texas lineages, and between Florida and the common ancestor of Main + Texas), (4) migration between geographically adjacent populations (i.e., no migration between Texas and Florida lineages), and (5) full isolation with migration model (migration permitted among all pairs of populations).

Following a series of preliminary analyses to identify optimal upper limits on uniform prior distributions for IMa3 analyses, we set the upper limit on divergence time priors as 7.0 and 15.0 for the divergences between the Texas and Main lineages, and Texas + Main and Florida, respectively. Prior limits on population sizes were set to 5.0 for the Texas lineage, and 20.0 for all other current and ancestral populations. Prior limits on migration rates were set to 2.0 between all current population pairs, and 5.0 for migration between the Florida lineage and the common ancestral population of the Texas + Main lineages. Two replicate analyses were run, each consisting of 40 chains with geometric heating parameters 0.98 and 0.65, following the authors' recommendations for small data sets under medium heating to achieve suitable mixing. Each chain was run for 20 million generations, sampling every 100 generations, following a burn-in period of 1 million generations, yielding a posterior sample of 200,000 samples. All posterior samples were then used to calculate joint posterior densities for comparison of nested models using likelihood ratio tests (Hey and Nielsen, 2007).

Genomic ddRAD Sequencing.—To further evaluate putative species boundaries and clades recovered in the Sanger sequencing analyses in a more genomically comprehensive context, we also used a double-digest restriction associated DNA sequencing (ddRADseq) for a small subset of the samples, representing all clades identified from Sanger-sequence analyses. A subsample of 13 samples of *O. aestivus*, spanning the distribution of the species and all lineages recovered in Sanger-data analyses, along with a single sample the sister species, *O. vernalis*, were sent to Floragenex, Inc. (Portland, Oregon, USA) for ddRADseq library

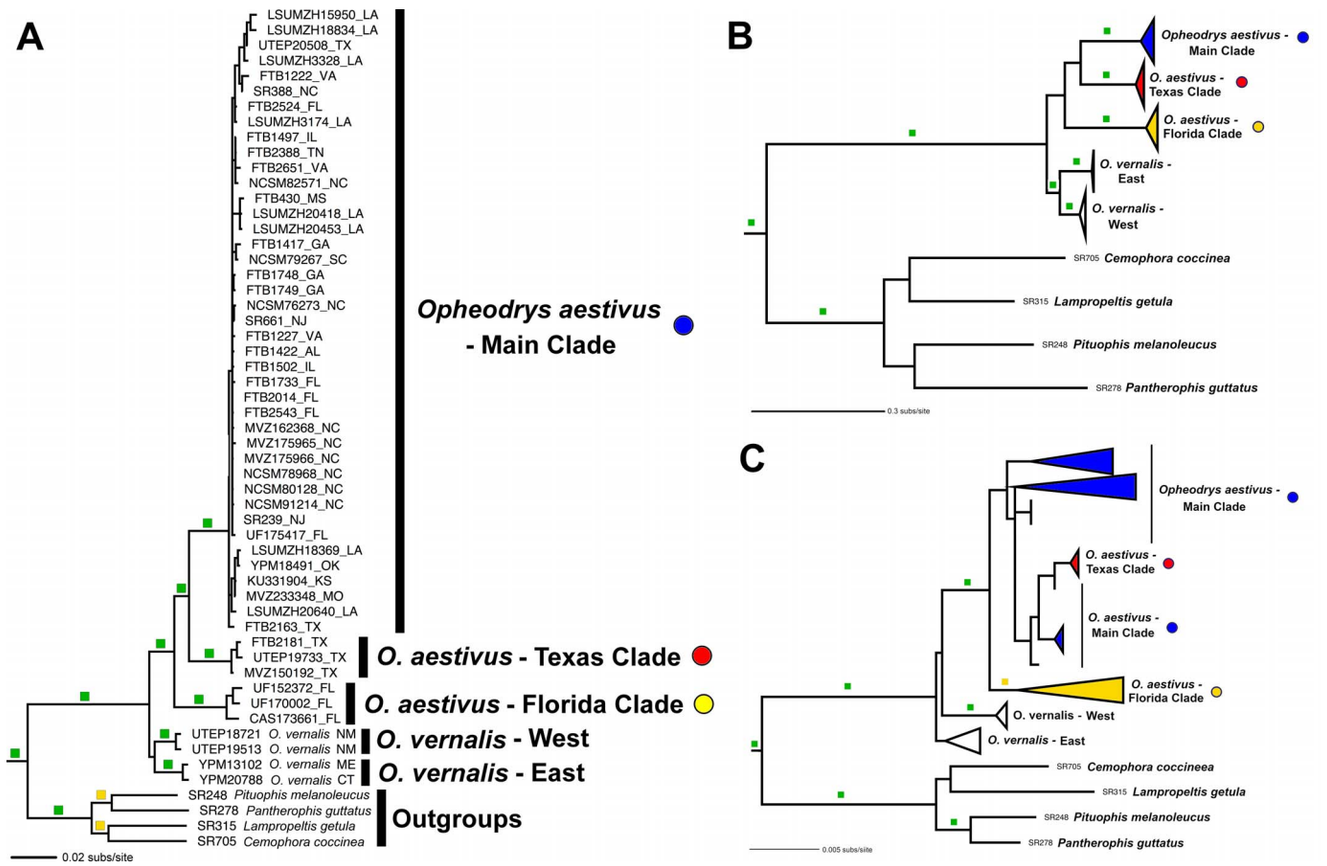

FIG. 2. (A) Bayesian maximum clade credibility phylogeny of *Opheodrys aestivus* based on partitioned analysis of concatenated Sanger loci. (B) Maximum likelihood phylogeny of *O. aestivus* from analysis of mitochondrial cytochrome b (cytb) data, partitioned by codon position. (C) Maximum likelihood phylogeny of *O. aestivus* based on concatenated analyses of three nuclear loci from Sanger sequence data, partitioned by locus. Symbols on nodes correspond to branch support values: green indicates Bayesian posterior probability (BPP) >0.95 and Maximum likelihood bootstrap (MLBS) >75, yellow indicates BPP >0.95 and MLBS <75. Symbols at branch tips correspond to the sampling localities in Fig. 1: yellow: peninsular Florida clade, red: central Texas clade, blue: Main clade.

preparation and sequencing (Appendix), and were included as part of 95 total samples sequenced on a single lane of an Illumina HiSeq 2500 platform. Resultant sequences were demultiplexed, stacks formed, and single nucleotide polymorphisms (SNPs) called in iPyRAD (Eaton and Overcast, 2020). Reads with over five low-quality base calls ($Q < 20$) and loci recovered from fewer than seven samples (50%) were discarded.

Phylogenomic Analyses.—We used Plink v. 2.0 (Chang et al., 2015) to calculate the number of private SNP alleles for each lineage recovered from Sanger sequence data, as well as to calculate pairwise Fst (Hudson et al., 1992) among these lineages. To visualize population genetic structure based on the SNP data, we used the adegenet v. 2.1.3 (Jombart, 2008; Jombart and Ahmed, 2011) package in Program R to conduct principal components analysis (PCA).

Both maximum likelihood and Bayesian inference were used to estimate the phylogeny of these samples from the ddRADseq dataset. RAxML was used to estimate the ML phylogeny using the full sequences, with 50 search replicates to find the ML phylogeny using the GTR+G model for each partition. Other parameters were left as default values, and 1,000 nonparametric bootstrap replicates were conducted to assess branch support. Bayesian analyses were conducted in Mr.Bayes, and were restricted to include only SNPs because of computational restrictions. Two independent runs of 4 chains were run for 12 million iterations each, sampling every 1,000 generations, the first 2,000 samples of which were discarded as burn-in. Stationarity and convergence were assessed via examining parameter trends and ESSs in Tracer.

We used SNAPP (SNP and AFLP Package for Phylogenetic analysis; Bryant et al., 2012) to estimate the species tree for *Opheodrys* using the genomic data, assuming the three clades found within *O. aestivus* (see results) as distinct lineages. Analyses were run for 6 million generations, sampling every 1,000 generations, the first 10% of which were discarded as burn-in. Parameter trends and ESSs were examined in Tracer to ensure chains had reached stationarity and sufficiently sampled the posterior.

RESULTS

The final concatenated alignment for the Sanger sequence data was 3,008 base-pairs (bp) in length (cytb = 1,117 bp, LAT = 795 bp, NT3 = 519 bp, PRLR = 577 bp), and 93.3% complete (82.1–100%/locus). Sequences were deposited in GenBank (Accession numbers: MZ080386–MZ080594); phased and unphased alignments are available via Dryad (Repository number: 10.5061/dryad.brv15dv8w).

Concatenated phylogenetic analyses (Fig. 2A) revealed strong support for the monophyly of the genus *Opheodrys* (MLBS = 100.0, BPP = 1.0), as well as for *O. aestivus s. l.* (MLBS = 92.9,

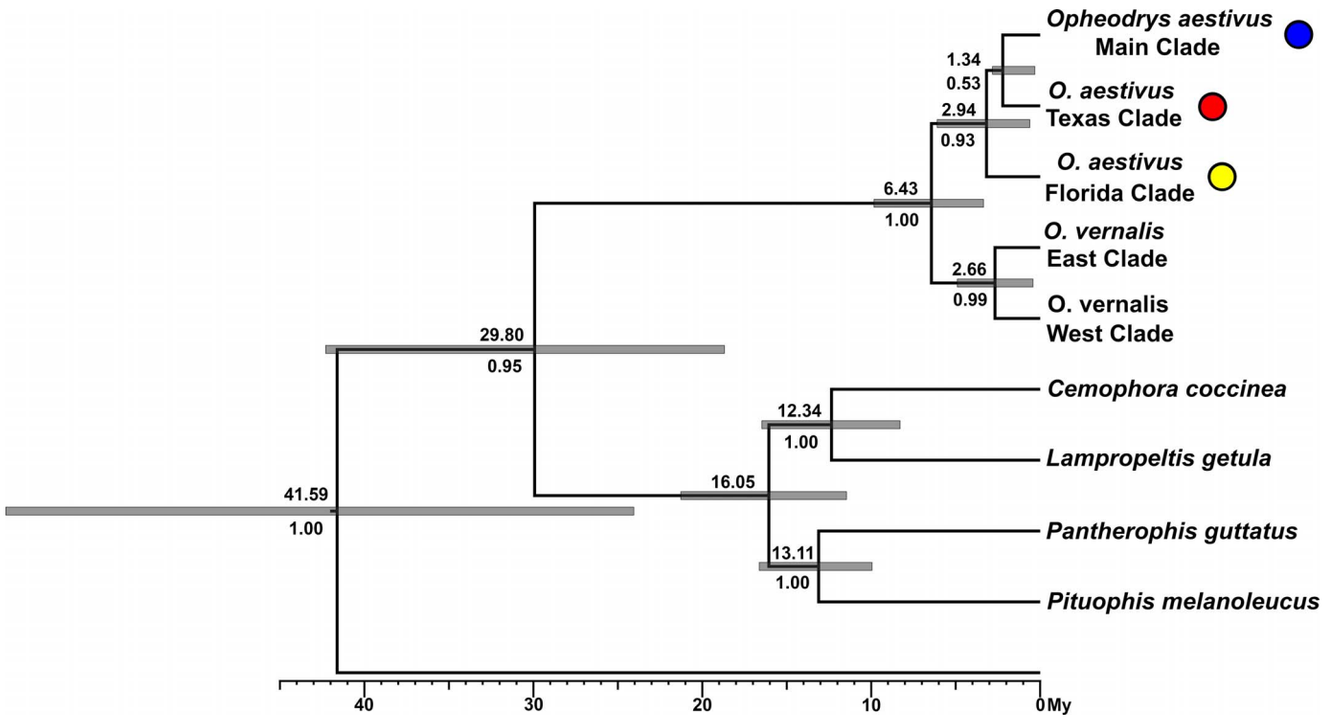

FIG. 3. Calibrated species tree for *Opheodrys aestivus* from Bayesian multispecies coalescent analyses of Sanger data in *BEAST. Fossil calibration points are indicated with asterisks. Values above branches indicate mean estimated node age in millions of years before present (mya), bars on nodes correspond to 95% credibility intervals. Values below branches correspond to BPP branch support. Colors of symbols at branch tips correspond to major clades in Figures 1 and 2.

BPP = 1.00). Within *O. aestivus s. l.*, we also recovered strong support for three clades: a peninsular Florida lineage (MLBS = 100.0, BPP = 1.00), a Texas lineage comprising samples from the Edwards Plateau of central Texas (MLBS = 100.0, BPP = 1.00), and a large "Main" lineage comprising the remaining samples, from east Texas to the Florida panhandle and to southern New Jersey (MLBS = 95.6, BPP = 1.00). Relationships among these clades were less well-resolved, but supported a sister relationship between the central Texas and Main clades (MLBS = 76.2, BPP = 0.995). Phylogenetic analyses of the mitochondrial data yielded similar results (Fig. 2B), with strong support for the monophyly of the genus *Opheodrys* (MLBS = 100, BPP = 1.00), the monophyly of *O. vernalis* (MLBS = 86.3, BPP = 0.98), and for each of the three major clades within *O. aestivus* (MLBS > 97.9, BPP = 1.00). However, relationships among these lineages were not resolved with strong support (MLBS < 46.6, BPP < 0.32). Concatenated phylogenetic analyses of nuclear data (Fig. 2C) strongly supported the monophyly of the genus *Opheodrys* (MLBS = 100, BPP = 1.00), and of *O. aestivus* (MLBS = 81, BPP = 0.999), and did recover the monophyly of the Florida clade, albeit without strong support in maximum likelihood analyses (MLBS = 35, BPP = 0.971). However, phylogenetic analyses of nuclear data were largely unresolved for *Opheodrys* beyond these lineages (Fig. 2C); individual gene genealogies were largely poorly supported, (available via Dryad Repository number: 10.5061/dryad.brv15dv8w).

Structure analyses of the complete *Opheodrys* data set identified two clusters using the ΔK method: one including the Main lineage of *O. aestivus*, and the second including all other samples of *O. aestivus* and *O. vernalis*. However, the Ln P(D) suggested four clusters, corresponding to the three clades of *O. aestivus* plus *O. vernalis*. This may, in part, be due to the substantially larger sample size for the Main clade relative to other clades identified in concatenated phylogenetic analyses (Figs. 1, 2), and so we subsequently reduced the Main clade to three samples via random subsampling to minimize the discrepancy in sample sizes, and reran the Structure analyses as described above; we found ΔK and Ln P(D) support four clusters when the Main clade is randomly subsampled to three samples. Independent analysis of samples included in the Main clade revealed no further clustering of samples, with extensive admixture between clusters detected for all values of $K > 1$. Analysis of only those samples included in the second cluster identified using the ΔK method supports three further clusters with no admixture via both ΔK and Ln P(D), corresponding to the central Texas and peninsular Florida lineages of *O. aestivus* and *O. vernalis*. Independent analysis of the *O. vernalis* samples revealed eastern and western *O. vernalis* as distinct clusters with no admixture. Combined, these analyses support a total of five clusters, corresponding to the three lineages within *O. aestivus s. l.* and to the eastern and western clades of *O. vernalis*, as identified in the concatenated phylogenetic analyses. Results of all Structure analyses are available via Dryad (Repository number: 10.5061/dryad.brv15dv8w).

Multispecies coalescent analyses in *BEAST yielded similar results to the concatenated phylogenetic analyses, with strong support (PP = 1.00) for the monophyly of the genus *Opheodrys*, and for the monophyly of *O. aestivus s. l.* (BPP = 0.93). However, relationships among the three major clades within *O. aestivus s. l.*, were unresolved (Fig. 3). Credibility intervals in divergence time estimates were relatively large (Fig. 3), likely as a result of the limited number of fossil calibrations and the lack of an informative fossil calibration within *Opheodrys*. However, we recovered an estimated divergence between *O. aestivus s. l.* and

TABLE 2. Maximized posterior density (log(P)), results of likelihood ratio tests, and estimates of migration among populations from testing of nested demographic models in IMa3. Asterisks in degrees of freedom (df) indicate the likelihood ratio test distribution is a mixture. Migration parameters enclosed in brackets were fixed to zero in the model. Populations are coded in the migration parameters as T: Texas Clade, M: Main Clade, F: Florida Clade, and A: ancestral Texas+Main.

Model	log(P)	df	2LLR	m_{TM}	m_{MT}	m_{TF}	m_{FT}	m_{MF}	m_{FM}	m_{FA}	m_{AF}
All migration parameters	11.32			0.0925	0.1241	0.0000	0.0165	0.0176	0.0000	0.3192	0.0000
No migration	11.32	8*	0	[0]	[0]	[0]	[0]	[0]	[0]	[0]	[0]
Main–Texas migration	0.05675	6*	22.52	0.0512	0.1416	[0]	[0]	[0]	[0]	[0]	[0]
Sister migration	5.283	4*	12.07	0.0000	0.1621	[0]	[0]	[0]	[0]	0.0547	0.0361
Adjacent migration	11.81	2*	−0.9873	0.0000	0.3666	[0]	[0]	0.0239	0.0000	0.4721	0.0000

O. vernalis of 6.43 (3.36 – 9.83) mya, reflecting a late Miocene divergence. Within *O. aestivus s. l.*, we recovered an estimated divergence of 1.34 (0.32–2.82) mya between the Main and Texas clades, reflecting a divergence in the early Pleistocene or near the Pliocene–Pleistocene border, and of 2.94 (0.61–6.09) mya between these clades and the Florida clade (Fig. 3), reflecting an earlier divergence in the Pliocene or early Pleistocene.

Coalescent analysis of isolation with migration models in IMa3 found the best fit demographic model to include migration between geographically adjacent taxa (i.e., between Texas and Main clades, between Main and Florida clades, and between Florida and Texas+Main clades) or no migration among lineages (Table 2). In the adjacent migration model that includes migration between the Florida and Main clades and in the full model including all migration parameters, the migration rate between the Florida clade and other clades is much lower than that between the Texas and Main clades (Table 2).

We recovered 20,691 loci (9,970–19,382/sample) via ddRADseq that passed filters, including 81,258 SNPs. Of these, 33,983 SNPs were recovered from all lineages identified from the Sanger sequence data, including 4,159 SNPs with private alleles restricted to the Florida clade, 10,583 SNPs with private alleles restricted to the Main clade, 2,437 SNPs with private alleles restricted to the Texas clade, and 9,268 SNPs with private alleles restricted to *O. vernalis* (Table 3). The PCA of the ddRADseq data supported substantial differentiation among the Sanger sequence–based clades. The first principal component (28.9% of variation) primarily showed differentiation between *O. aestivus* and *O. vernalis*, while the second and third principal components (12.4% and 10.5% of variation, respectively) revealed strong differentiation of the Florida and Texas clades from each other and from the *O. aestivus* Main clade and *O. vernalis* (Fig. 4).

The data set included 18,582 SNPs that were independent (i.e., from different loci) and biallelic, and thus suitable for, and used in, SNAPP species-tree analyses. Raw ddRADseq reads and alignments of filtered loci are available via Dryad (Repository number: 10.5061/dryad.brv15dv8w).

TABLE 3. Genetic divergence among clades of *Opheodrys aestivus* (Florida, Main, Texas) and *O. vernalis*. Numbers above diagonal indicate mean uncorrected p-distance based on cytb sequences. Numbers below diagonal indicate the pairwise Fst based on ddRADseq data. Numbers on diagonal indicate the number of SNPs private to each clade.

	Florida	Main	Texas	*O. vernalis*
Florida	4,159	0.0992	0.0994	0.0938
Main	0.6125	10,583	0.0800	0.0915
Texas	0.7296	0.4914	2,437	0.0851
O. vernalis	0.7561	0.6941	0.7687	9,268

Concatenated phylogenomic analyses of ddRADseq data strongly corroborate results of Sanger data-based analyses (Fig. 5). The monophyly of *O. aestivus* was strongly supported (MLBS = 100, BPP = 1.00), as was that of the Main clade (MLBS = 100, BPP = 1.00), and for the sister relationship between the Main and Texas clades (MLBS = 100, BPP = 1.00). Species-tree analyses in SNAPP corroborated other analyses with respect to high support for a sister relationship between the Main and Texas clades (BPP = 1.0; Fig. 5). However, as in the species-tree analyses based on Sanger data, the relationships between the Main + Texas clades, the Florida clade, and *O. vernalis* were not well-supported (BPP = 0.62).

DISCUSSION

The divergence between the peninsular Florida populations and other populations is not surprising, given the morphological differences between these clades and the long history of documented phylogeographic breaks between peninsular Florida and the rest of continental North America in a wide variety of taxa. Similar breaks were documented in some of the earliest phylogeographic studies (Avise et al., 1987; Avise, 2000), and have been reported in a wide variety of terrestrial taxa (Avise et al., 1987; Swenson and Howard, 2005; Seal et al., 2015; Fetter and Weakley, 2019), including amphibians (Austin et al., 2002; Means et al., 2017; Barrow et al., 2018), turtles (Walker et al., 1998a,b), squamates (Burbrink et al., 2008; Fontanella et al., 2008; Manthey et al., 2016; McKelvy and Burbrink, 2017), birds (Barrowclough et al., 2018, 2019), and mammals (Avise et al., 1987; Ellsworth et al., 1994; Jackson and Cook, 2020). Many of these studies did not estimate divergence time between divergent peninsular Florida populations and other populations from continental North America, but some of those have found similar divergence times to the 2.94 (0.61–6.09) mya divergence we recovered in *O. aestivus*. Fontanella et al. (2008) estimated a divergence time of 2.721 (0.95–4.88) mya between the peninsular Florida clade and clades from further north in continental North America in the snake *Diadophis punctatus*, and Manthey et al. (2016) found that other continental North American populations of *Anolis carolinensis* diverged from the most closely related of several clades restricted to peninsular Florida 2.78 (2.30–3.41) mya. Other taxa have shown much older divergences (6.183 [3.163–9.667] mya in *Coluber constrictor;* Burbrink et al., 2008), or potentially much younger divergences (albeit without published date estimates, e.g., in turtles [Walker et al., 1998b] and birds [Barrowclough et al., 2019]). Combined, these shared geographic patterns of divergence make it clear that the history of peninsular Florida, either as a single event or as a result of multiple waves of divergence, is an important factor that has played a major role in the evolutionary and biogeographic history of much of North American biota.

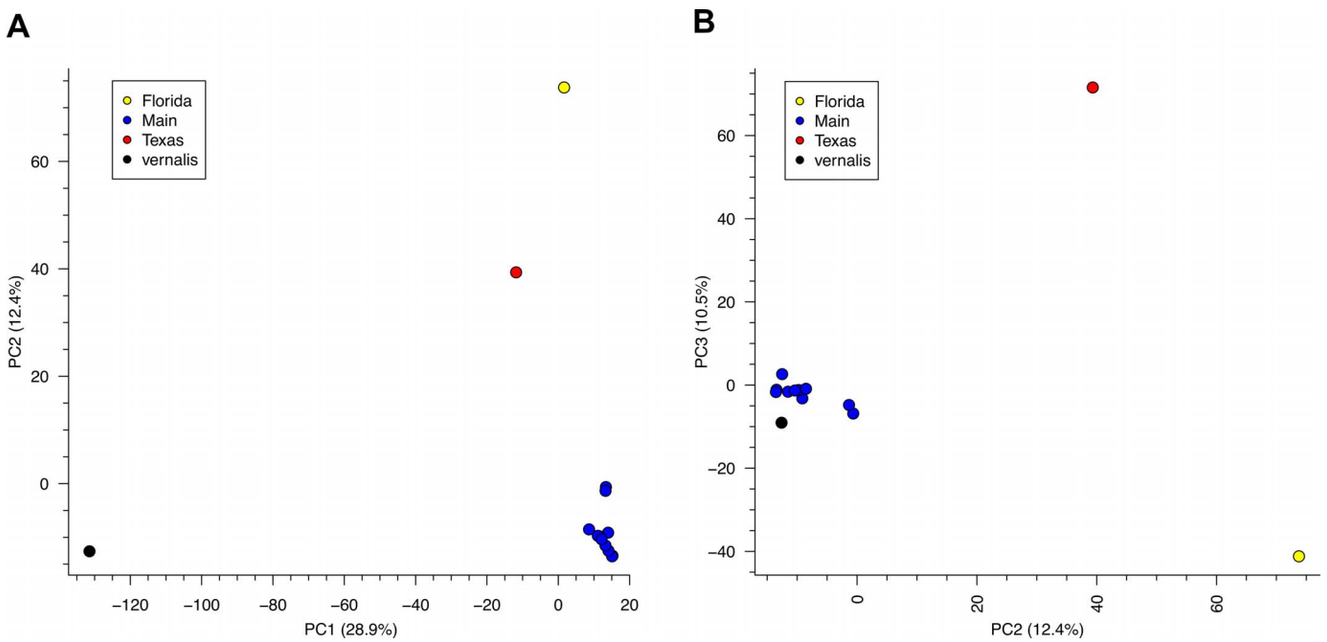

FIG. 4. Plots from principal components analysis of SNPs from ddRADseq data. (A) PC1 (28.9% of variation) vs. PC2 (12.4%), and (B) PC2 vs. PC3 (10.5%). Colors correspond to major clades as indicated in Figures 1 and 2: yellow: Florida clade, blue: Main clade, red: Texas clade, and black: *O. vernalis*.

The lack of structure within the Main *O. aestivus* clade, however, is less expected, because we found little to no divergence among populations from the Texas Gulf Coast, east to the Florida panhandle, and north to southern New Jersey (Figs. 1, 2). Most squamates show substantial population structure in this region, at least across major barriers or ecological transitions such as the Mississippi River and/or as habitat changes from eastern deciduous forest to grasslands (e.g., *Coluber constrictor* [Burbrink et al., 2008]; *Lampropeltis getula* complex [Pyron and Burbrink, 2009b; Krysko et al., 2017]; *Lampropeltis triangulum* complex [Ruane et al., 2014]; *Pantherophis guttatus* complex [Burbrink, 2002; Myers et al., 2020]; *Pantherophis obsoletus* complex [Burbrink et al., 2000, 2021; Burbrink, 2001]; *Sceloporus undulatus* complex [Leaché and Reeder, 2002]). Many squamates also show more fine-scale phylogeographic structure within this region (e.g., *Diadophis punctatus* [Fontanella et al., 2008]; *Scincella lateralis* [Jackson and Austin, 2012]). However, our observed pattern of phylogeographic structure is not unique to *O. aestivus*. The Scarletsnake, *Cemophora coccinea*, similarly shows limited population structure across the region from western Louisiana to southern New Jersey (Weinell and Austin, 2017). Thus, our data suggest that while many species may have persisted in, and expanded from, multiple Pleistocene refugia, others, including *C. coccinea* and *O. aestivus*, may have recolonized northern regions primarily from single refugia in the postglacial period. Additional research should focus on the ecological similarities between those taxa that have apparently expanded from a single refugium following Pleistocene glacial retreat versus those that apparently expanded from multiple refugia, or test whether these differences are merely a result of stochasticity.

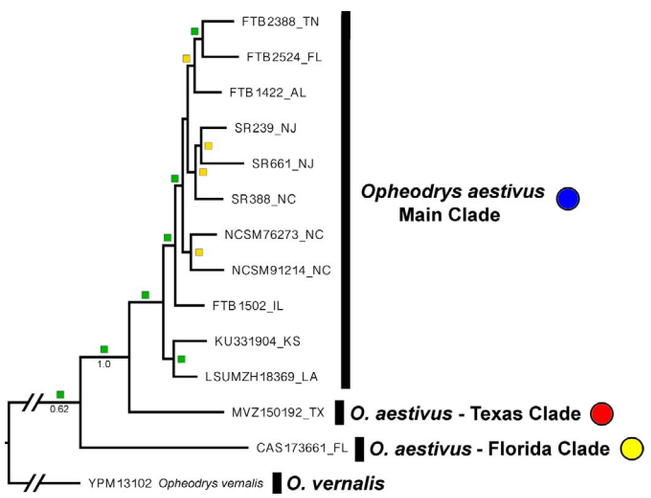

FIG. 5. Bayesian maximum clade credibility phylogeny of *Opheodrys aestivus* based on ddRADseq data. Symbols on nodes correspond to branch support values: green indicates Bayesian posterior probability (BPP) >0.95 and Maximum likelihood bootstrap (MLBS) >75, yellow indicates BPP >0.95 and MLBS <75. Values below branches indicate BPP support from species tree analysis of ddRADseq data in SNAPP. Colors of symbols at branch tips correspond to the sampling localities in Figs. 1 and 2. ls correspond to those listed in the Appendix.

We found evidence for an additional clade, perhaps even a distinct species, that appears restricted to the Edwards Plateau region of Texas and may have become isolated during Pleistocene glacial cycles, based on our estimated divergence time of 1.99 (0.30–2.62) mya. The Edwards Plateau is a unique ecosystem that occurs at the confluence of the Gulf Coast, Great Plains, and Chihuahuan Desert biomes, and represents the northeastern-most portion of the distributions of several primarily Mexican species (e.g., *Thamnophis cyrtopsis*, *Gerrhonotus infernalis*; Webb, 1980; Powell et al., 2016). Numerous other taxa with broad distributions across eastern North America similarly have clades restricted to this region, including *Pantherophis bairdi* in the *P. obsoletus* complex (Burbrink et al., 2000; Burbrink, 2001), *Agkistrodon laticinctus* in the *A. contortrix* complex (Burbrink and Guiher, 2015), and some clades of

Scincella lateralis (Jackson and Austin, 2010), among others (Baird et al., 2006; Rodriguez et al., 2012; Thomson et al., 2018). Although estimates of the divergence times of these other lineages restricted to the Edwards Plateau are limited, these data support the importance of this region as a possible Pleistocene refugium for numerous disparate taxa, and its importance in driving the generation of diversity in taxa currently broadly distributed across eastern North America.

Taxonomic Treatment.—Our analyses recover a deep and strongly supported divergence between the populations of *O. aestivus s. l.* from peninsular Florida and all other *O. aestivus* populations, with our estimates suggesting this lineage diverged from the rest of *O. aestivus s. l.* nearly 3 mya, during the late Pliocene (Figs. 2, 3). Further, demographic analyses of isolation with migration models find that migration between this peninsular Florida population and other populations of *O. aestivus* is either excluded from the model or very low (Table 2). This clade is represented by a limited sample size (Florida clade $n = 3$), but these samples span the northern and southern extremes of the Florida peninsula (Fig. 1), and the northern-most sample in this clade is <100 km from samples in the Main clade (mean cytb uncorrected p-distance = 0.099). This is further supported via previously published morphological studies with geographic sampling that appears to correspond with distinctness of this lineage. Grobman (1984) recognized the subspecies *O. a. aestivus,* with a type locality of 1 mile west of Parksville, McCormick Co., South Carolina (well within the distribution of the Main clade we recovered), as including the majority of the eastern North American populations of *O. aestivus,* but found that peninsular Florida populations had more strongly keeled scales, and that the keels extended laterally to the third dorsal scale row, although it is worth noting that squamate scales are known to vary within species across their geographic ranges (e.g., *Natrix tessellata*; Mebert, 2011). Based on his results, Grobman (1984) described these peninsular Florida populations as the subspecies *O. a. carinatus,* the type locality of which is Archibold Biological Station, Highlands Co., Florida. Further, Plummer (1987) found the peninsular Florida populations to be larger in mean and maximum size relative to other populations of *O. aestivus*. Combining evidence from our results and these previously published studies, we suggest that the peninsular Florida populations be elevated to species status, encompassing the former subspecies *O. a. carinatus* and to be recognized as *Opheodrys carinatus* Grobman 1984 *stat. nov.*

We also find the central Texas populations from the Edwards Plateau as distinct and diverging from the Main clade of *O. aestivus* near the Pliocene–Pleistocene boundary (Figs. 2, 3). It is possible this is the same entity as the previously described subspecies *O. a. majalis,* in part, as recognized by Grobman (1984). However, the type locality of *majalis* is in Indianola, Texas, on the Texas Gulf Coast, a different ecoregion to the Edwards Plateau, to which our data suggest this clade may be restricted, and our other Gulf Coast sampling from further east are within the Main *O. aestivus* clade (Figs. 1, 2). Further, previous morphological studies have found far less distinctive differences between these populations and the rest of *O. aestivus,* relying largely on broadly overlapping differences in the number of ventral and subcaudal scales (Grobman, 1984). As such, we refrain from elevating the central Texas clade to any specific status pending denser molecular sampling that can better refine the distribution of this clade, determine its status as a distinct species, and elucidate whether this clade perhaps represents *majalis* as distinct or a wholly undescribed lineage. At this time, we recommend that no subspecies be recognized for *O. aestivus* because we found no evidence that they (*O. a. majalis, O. a. conanti*) represent any clearly recognizable evolutionary entities, and suggest that *O. vernalis, O. aestivus,* and *O. carinatus* best characterize the diversity found within *Opheodrys* based on currently available information.

Conclusions.—Our data show that, despite having previously been considered a single broadly distributed species, *O. aestivus* is likely a complex of at least two species: a peninsular Florida species; a broadly distributed eastern North American species; and, potentially, a third species in central Texas. Our results display an unusual combination of patterns found in other taxa. The divergence of peninsular Florida has long been a documented pattern, and several taxa or lineages are restricted to central Texas, yet few other squamates show such low levels of divergence from east Texas to the Florida panhandle and north to New Jersey.

Our approach also illustrates how dense geographic sampling can be used as a guide for selecting samples for more comprehensive genomic sequencing as a cost-effective means of combining intense geographic and genomic sampling. Finally, we recover identical phylogenies and similar support values and relative branch lengths based on Sanger and ddRADseq data, suggesting that while there are certainly situations where genomic data is necessary, particularly in taxa with short internodes or introgression, a small number of loci may, in some cases, be used to resolve phylogeographic or phylogenetic questions as effectively as genomic sampling.

Acknowledgments.—We thank F. Burbrink, C. Raxworthy, and D. Kizirian (AMNH); L. Scheinberg (CAS); R. Brown, R. Glor, and L. Welton (KU); C. Austin, R. Brumfield, D. Dittmann, and F. Sheldon (LSUMZ); J. McGuire and C. Spencer (MVZ); B. Stuart and J. Beane (NCSM); D. Blackburn and C. Sheehy III (UF); E. Greenbaum, J. D. Johnson, C. S. Lieb, and V. M. Zhuang (UTEP); and G. Watkins-Colwell and J. Gauthier (YPM) for providing tissue loans. We also thank K. Schantz, B. Zarate, L. DiPiano, the New Jersey Department of Environmental Protection, and the New Jersey Division of Fish and Wildlife for providing permits (permit numbers: SW 2017040 and SW 2018011). This research was conducted under Rutgers University – Newark IACUC protocol number 17040A1. We thank J. Boone and J. Walsh for assistance with ddRAD sequencing at Floragenex, and I. Overcast on the use of iPyRAD for processing ddRAD sequences. We also thank J. Bernstein for his assistance and discussions regarding the project.

Literature Cited

Austin, J. D., S. C. Lougheed, L. Neidrauer, A. A. Chek, and P. T. Boag. 2002. Cryptic lineages in a small frog: the post-glacial history of the spring peeper, *Pseudacris crucifer* (Anura: Hylidae). Molecular Phylogenetics and Evolution 25:316–329. doi: 10.1016/S1055-7903(02)00260-9.

Avise, J. C. 2000. Phylogeography: The History and Formation of Species. Harvard University Press, USA.

Avise, J. C., J. Arnold, R. M. Ball, E. Bermingham, T. Lamb, J. E. Neigel, C. A. Reeb, and N. C. Saunders. 1987. Intraspecific phylogeography: the mitochondrial DNA bridge between population genetics and wystematics. Annual Review of Ecology and Systematics 18:489–522.

Baird, A. B., J. K. Krejca, J. R. Reddell, C. E. Peden, M. J. Mahoney, and D. M. Hillis. 2006. Phylogeographic structure and color pattern variation among populations of *Plethodon albagula* on the Edwards Plateau of Central Texas. Copeia 2006:760–768. doi: 10.1643/0045-8511(2006)6.

Barrow, L. N., A. R. Lemmon, and E. M. Lemmon. 2018. Targeted sampling and target capture: assessing phylogeographic concordance with genome-wide data. Systematic Biology 67:979–996. doi: 10.1093/sysbio/syy021.

Barrowclough, G. F., J. G. Groth, E. K. Bramlett, J. E. Lai, and W. M. Mauck. 2018. Phylogeography and geographic variation in the red-bellied woodpecker (*Melanerpes carolinus*): characterization of mtDNA and plumage hybrid zones. The Wilson Journal of Ornithology 130:671–683. doi: 10.1676/17-070.1.

Barrowclough, G. F., J. G. Groth, W. M. Mauck, and M. E. Blair. 2019. Phylogeography and species limits in the red-shouldered hawk (*Buteo lineatus*): characterization of the Northern Florida Suture Zone in birds. Ecology and Evolution 9:6245–6258. doi: 10.1002/ece3.5190.

Bickford, D., D. J. Lohman, N. S. Sodhi, P. K. L. Ng, R. Meier, K. Winker, K. K. Ingram, and I. Das. 2007. Cryptic species as a window on diversity and conservation. Trends in Ecology & Evolution 22:148–155. doi: 10.1016/j.tree.2006.11.004.

Bortolus, A. 2008. Error cascades in the biological sciences: the unwanted consequences of using bad taxonomy in ecology. Ambio 37:114–118.

Bouckaert, R., J. Heled, D. Kühnert, T. Vaughan, C. H. Wu, D. Xie, M. A. Suchard, A. Rambaut, and A. J. Drummond. 2014. BEAST 2: a software platform for Bayesian evolutionary analysis. PLOS Computational Biology 10:1–6. doi: 10.1371/journal.pcbi.1003537.

Bryant, D., R. Bouckaert, J. Felsenstein, N. A. Rosenberg, and A. RoyChoudhury. 2012. Inferring species trees directly from biallelic genetic markers: bypassing gene trees in a full coalescent analysis. Molecular Biology and Evolution 29:1917–1932. doi: 10.1093/molbev/mss086.

Burbrink, F. T. 2001. Systematics of the eastern ratsnake complex (*Elaphe obsoleta*). Herpetological Monographs 15:1–53.

———. 2002. Phylogeographic analysis of the corn snake (*Elaphe guttata*) complex as inferred from maximum likelihood and Bayesian analyses. Molecular Phylogenetics and Evolution 25:465–476.

Burbrink, F. T., and T. J. Guiher. 2015. Considering gene flow when using coalescent methods to delimit lineages of North American pitvipers of the genus *Agkistrodon*. Zoological Journal of the Linnean Society 173:505–526. doi: 10.1111/zoj.12211.

Burbrink, F. T., F. Fontanella, R. Alexander Pyron, T. J. Guiher, and C. Jimenez. 2008. Phylogeography across a continent: the evolutionary and demographic history of the North American racer (Serpentes: Colubridae: *Coluber constrictor*). Molecular Phylogenetics and Evolution 47:274–288. doi: 10.1016/j.ympev.2007.10.020.

Burbrink, F. T., R. Lawson, and J. B. Slowinski. 2000. Mitochondrial DNA phylogeography of the polytypic North American Rat Snake (*Elaphe obsoleta*): a critique of the subspecies concept. Evolution 54:2107–2118.

Burbrink, F. T., M. Gehara, A. D. McKelvy, E. A. Myers. 2021. Resolving spatial complexities of hybridization in the context of the gray zone of speciation in North American ratsnakes (*Pantherophis obsoletus* complex). Evolution: In press.

Chang, C. C., C. C. Chow, L. C. A. M. Tellier, S. Vattikuti, S. M. Purcell, and J. J. Lee. 2015. Second-generation PLINK: rising to the challenge of larger and richer datasets. Gigascience 4:s13742–015-0047-8. doi: 10.1186/s13742-015-0047-8.

Coyne, J. A., and H. A. Orr. 2004. Speciation. Sinauer Associates, Inc., USA.

Crother, B. I., M. E. White, J. M. Savage, M. E. Eckstut, M. R. Graham, and. D. W. Gardner. 2011. A reevaluation of the status of the foxsnakes *Pantherophis gloydi* Conant and *P. vulpinus* Baird and Girard (Lepidosauria). ISRN Zoology 2011:1–15.

D'Amen, M., N. E. Zimmermann, and P. B. Pearman. 2013. Conservation of phylogeographic lineages under climate change. Global Ecology and Biogeography 22:93–104. doi: 10.1111/j.1466-8238.2012.00774.x.

DiLeo, M. F., J. D. Rouse, J. A. Dávila, and S. C. Lougheed. 2013. The influence of landscape on gene flow in the eastern massassauga rattlesnake (*Sistrurus c. catenatus*): insight from computer simulations. Molecular Ecology 22:4483–4498. doi: 10.1111/mec.12411.

Earl, D. A., and B. M. VonHoldt. 2012. STRUCTURE HARVESTER: a website and program for visualizing STRUCTURE output and implementing the Evanno method. Conservation Genetics Resources 4:359–361. doi: 10.1007/s12686-011-9548-7.

Eaton, D. A. R., and I. Overcast. 2020. ipyrad: interactive assembly and analysis of RADseq datasets. Bioinformatics btz966. doi: 10.1093/bioinformatics/btz966.

Edgar, R. C. 2004. MUSCLE: multiple sequence alignment with high accuracy and high throughput. Nucleic Acids Research 32:1792–1797. doi: 10.1093/nar/gkh340.

Edwards, S. V, L. Liu, and D. K. Pearl. 2007. High-resolution species trees without concatenation. Proceedings of the National Academy of Sciences of the United States of America 104:5936–5941.

Ellsworth, D. L., R. L. Honeycutt, N. J. Silvy, J. W. Bickham, and W. D. Klimstra. 1994. Historical biogeography and contemporary patterns of mitochondrial DNA variation in white-tailed deer from the Southeastern United States. Evolution 48:122–136.

Evanno, G., S. Regnaut, and J. Goudet. 2005. Detecting the number of clusters of individuals using the software Structure: a simulation study. Molecular Ecology 14:2611–2620.

Falush, D., M. Stephens, and J. K. Pritchard. 2003. Inference of population structure using multilocus genotype data: linked loci and correlated allele frequencies. Genetics 164:1567–1587.

Fetter, K. C., and A. Weakley. 2019. Reduced gene flow from mainland populations of *Liriodendron tulipifera* into the Florida peninsula promotes diversification. International Journal of Plant Sciences 180:253–269. doi: 10.1086/702267.

Fontanella, F. M., C. R. Feldman, M. E. Siddall, and F. T. Burbrink. 2008. Phylogeography of *Diadophis punctatus*: extensive lineage diversity and repeated patterns of historical demography in a trans-continental snake. Molecular phylogenetics and evolution 46:1049–1070. doi: 10.1016/j.ympev.2007.10.017.

Frost, D. R., and D. M. Hillis. 1990. Species in concept and practice: herpetological applications. Herpetologica 46:87–104.

Frost, D. R., A. G. Kluge, and D. M. Hillis. 1992. Species in contemproary herpetology: comments on phylogenetic inference and taxonomy. Herpetological Review 23:46–54.

Grobman, A. B. 1984. Scutellation variation in *Opheodrys aestivus*. Bulletin of the Florida State Museum, Biological Sciences 29:153–170.

Guyer, C., C. Murray, H. L. Bart, B. I. Crother, R. E. Chabarria, M. A. Bailey, and K. Dunn. 2020. Colour and size reveal hidden diversity of *Necturus* (Caudata: Proteidae) from the Gulf Coast Plain of the United States. Journal of Natural History 54:15–41.

Hammerson, G. A., P. Lavin, and F. Mendoza Quijano. 2007. *Opheodrys aestivus*. The IUCN Red List of Threatened Species e.T63859A1. doi: 10.2305/IUCN.UK.2007.RLTS.T63859A12722881.en.

Head, J. J., K. Mahlow, and J. Müller. 2016. Fossil calibration dates for molecular phylogenetic analysis of snakes 2: Caenophidia, Colubroidea, Elapoidea, Colubridae. Paleontologica Electronica 19.2.2FC. doi: 10.26879/625.

Heled, J., and A. J. Drummond. 2010. Bayesian inference of species trees from multilocus data. Molecular Biology and Evolution 27:570–580. doi: 10.1093/molbev/msp274.

Hey, J. 2010. Isolation with migration models for more than two populations. Molecular Biology and Evolution 27:905–920. doi: 10.1093/molbev/msp296.

Hey, J., and R. Nielsen. 2004. Multilocus methods for estimating population sizes, migration rates and divergence time, with applications to the divergence of *Drosophila pseudoobscura* and *D. persimilis*. Genetics 167:747–760. doi: 10.1534/genetics.103.024182.

———, and ———. 2007. Integration within the Felsenstein equation for improved Markov chain Monte Carlo methods in population genetics. Proceedings of the National Academy of Sciences of the United States of America 104:2785–2790. doi: 10.1073/pnas.0611164104.

Hey, J., Y. Chung, A. Sethuraman, J. Lachance, S. Tishkoff, V. C. Sousa, and Y. Wang. 2018. Phylogeny estimation by integration over isolation with migration models. Molecular Biology and Evolution 35:2805–2818. doi: 10.1093/molbev/msy162.

Hickerson, M. J., B. C. Carstens, J. Cavender-Bares, K. A. Crandall, C. H. Graham, J. B. Johnson, L. Rissler, P. F. Victoriano, and A. D. Yoder. 2010. Phylogeography's past, present, and future: 10 years after Avise, 2000. Molecular Phylogenetics and Evolution 54:291–301. doi: 10.1016/j.ympev.2009.09.016.

Holman, J. A. 2000. Fossil Snakes of North America: Origin, Evolution, Distribution, Paleoecology. Indiana University Press, USA.

Hudson, R. R., M. Slatkin, and W. P. Maddison. 1992. Estimation of levels of gene flow from DNA sequence data. Genetics 132:583–589.

Huelsenbeck, J. P., and F. Ronquist. 2001. MrBayes: Bayesian inference of phylogenetic trees. Bioinformatics 17:754–755. doi: 10.1093/bioinformatics/17.8.754.

Isaac, N. J. B., J. Mallet, and G. M. Mace. 2004. Taxonomic inflation: its influence on macroecology and conservation. Trends in Ecology & Evolution 19:464–469.

Jackson, D. J., and J. A. Cook. 2020. A precarious future for distinctive peripheral populations of meadow voles (*Microtus pennsylvanicus*). Journal of Mammalogy 101:36–51. doi: 10.1093/jmammal/gyz196.

Jackson, N. D., and C. C. Austin. 2010. The combined effects of rivers and refugia generate extreme cryptic fragmentation within the common ground skink (*Scincella lateralis*). Evolution 64:409–428. doi: 10.1111/j.1558-5646.2009.00840.x.

———, and ———. 2012. Inferring the evolutionary history of divergence despite gene flow in a lizard species, *Scincella lateralis* (Scincidae), composed of cryptic lineages. Biological Journal of the Linnean Society 107:192–209. doi: 10.1111/j.1095-8312.2012.01929.x.

Jombart, T. 2008. adegenet: a R package for the multivariate analysis of genetic markers. Bioinformatics 24:1403–1405. doi: 10.1093/bioinformatics/btn129.

Jombart, T., and I. Ahmed. 2011. adegenet 1.3-1: new tools for the analysis of genome-wide SNP data. Bioinformatics 27:3070–3071. doi: 10.1093/bioinformatics/btr521.

Kajtoch, Ł., E. Cieślak, Z. Varga, W. Paul, M. A. Mazur, G. Sramkó, and D. Kubisz. 2016. Phylogeographic patterns of steppe species in Eastern Central Europe: a review and the implications for conservation. Biodiversity and Conservation 25:2309–2339. doi: 10.1007/s10531-016-1065-2.

Kearse, M., R. Moir, A. Wilson, S. Stones-Havas, M. Cheung, S. Sturrock, S. Buxton, A. Cooper, S. Markowitz, C. Duran, T. Thierer, B. Ashton, P. Meintjes, and A. Drummond. 2012. Geneious Basic: an integrated and extendable desktop software platform for the organization and analysis of sequence data. Bioinformatics 28:1647–1649. doi: 10.1093/bioinformatics/bts199.

Kopelman, N. M., J. Mayzel, M. Jakobsson, N. A. Rosenberg, and I. Mayrose. 2015. CLUMPAK: a program for identifying clustering modes and packaging population structure inferences across *K*. Molecular Ecology Resources 15:1179–1191. doi: 10.1111/1755-0998.12387.

Krysko, K. L., L. P. Nuñez, C. E. Newman, and B. W. Bowen. 2017. Phylogenetics of kingsnakes, *Lampropeltis getula* complex (Serpentes: Colubridae), in eastern North America. Journal of Heredity 108:226–238. doi: 10.1093/jhered/esw086.

Kumar, R., and V. Kumar. 2018. A review of phylogeography: biotic and abiotic factors. Geology, Ecology, and Landscapes 2:268–274. doi: 10.1080/24749508.2018.1452486.

Lait, L. A., and P. D. N. Hebert. 2018. A survey of molecular diversity and population genetic structure in North American clearwing moths (Lepidoptera: Sesiidae) using cytochrome c oxidase I. PLoS ONE 13:6–8. doi: 10.1371/journal.pone.0202281.

Leaché, A. D., and T. W. Reeder. 2002. Molecular systematics of the Eastern Fence Lizard (*Sceloporus undulatus*): a comparison of parsimony, likelihood, and Bayesian approaches. Systematic Biology 51:44–68.

Lemmon, E. M., A. R. Lemmon, J. T. Collins, J. A. Lee-Yaw, and D. C. Cannatella. 2007. Phylogeny-based delimitation of species boundaries and contact zones in the trilling chorus frogs (*Pseudacris*). Molecular Phylogenetics and Evolution 44:1068–1082. doi: 10.1016/j.ympev.2007.04.010.

Luna-Aranguré, C., and E. Vázquez-Domínguez. 2020. Analysis of the application of ecological niche modeling in phylogeographic studies: contributions, challenges, and future. Therya 11:47–55. doi: 10.12933/therya-20-844.

Manthey, J. D., M. Tollis, A. R. Lemmon, E. Moriarty Lemmon, and S. Boissinot. 2016. Diversification in wild populations of the model organism *Anolis carolinensis*: a genome-wide phylogeographic investigation. Ecology and Evolution 6:8115–8125. doi: 10.1002/ece3.2547.

Mascarenhas, R., C. Y. Miyaki, R. Dobrovolski, and H. Batalha-Filho. 2019. Late Pleistocene climate change shapes population divergence of an Atlantic Forest passerine: a model-based phylogeographic hypothesis test. Journal of Ornithology 160:733–748. doi: 10.1007/s10336-019-01650-1.

McCormack, J. E., J. Heled, K. S. Delaney, A. T. Peterson, and L. L. Knowles. 2011. Calibrating divergence times on species trees versus gene trees: implications for speciation history of Aphelocoma jays. Evolution 65:184–202. doi: 10.1111/j.1558-5646.2010.01097.x.

McKelvy, A. D., and F. T. Burbrink. 2017. Ecological divergence in the yellow-bellied kingsnake (*Lampropeltis calligaster*) at two North American biodiversity hotspots. Molecular Phylogenetics and Evolution 106:61–72. doi: 10.1016/j.ympev.2016.09.006.

Means, D. B., J. Y. Lamb, and J. Bernardo. 2017. A new species of dusky salamander (Amphibia: Plethodontidae: *Desmognathus*) from the Eastern Gulf coastal plain of the United States and a redescription of *D. auriculatus*. Zootaxa 4263:467–506. doi: 10.11646/zootaxa.4263.3.3.

Mebert, K. 2011. Geographic variation of morphological characters in the dice snake (*Natrix tessellata*). Mertensiella 18:11–20.

Médail, F., and A. Baumel. 2018. Using phylogeography to define conservation priorities: the case of narrow enndemic plants in the Mediterrannean Basin hotspot. Biological Conservation 224:258–266. doi: 10.1016/j.biocon.2018.05.028.

Myers, E. A., A. D. McKelvy, and F. T. Burbrink. 2020. Biogeographic barriers, Pleistocene refugia, and climatic gradients in the southeastern Nearctic drive diversification in cornsnakes (*Pantherophis guttatus* complex). Molecular Ecology 29:797–811. doi: 10.111/mec.15358.

Nadeau, C. P., and M. C. Urban. 2019. Eco-evolution on the edge during climate change. Ecography 42:1280–1297. doi: 10.1111/ecog.04404.

Noonan, B. P., and P. T. Chippindale. 2006. Dispersal and vicariance: the complex evolutionary history of boid snakes. Molecular Phylogenetics and Evolution 20:347–358. doi: 10.1016/j.ympev.2006.03.010.

Papadopoulou, A., and L. L. Knowles. 2016. Toward a paradigm shift in comparative phylogeography driven by trait-based hypotheses. Proceedings of the National Academy of Sciences of the United States of America 113:8018–8024. doi: 10.1073/pnas.1601069113.

Plummer, M. V. 1987. Geographic variation in body size of green snakes (*Opheodrys aestivus*). Copeia 1987:483–485. doi: 10.2307/1445787.

Polfus, J. L., M. Manseau, C. F. C. Klütsch, D. Simmons, and P. J. Wilson. 2017. Ancient diversification in glacial refugia leads to intraspecific diversity in a Holarctic mammal. Journal of Biogeography 44:386–396. doi: 10.1111/jbi.12918.

Posada, D. 2008. jModelTest: phylogenetic model averaging. Molecular Biology and Evolution 25:1253–1256. doi: 10.1093/molbev/msn083.

Powell, R., R. Conant, and J. T. Collins. 2016. Field Guide to Reptiles and Amphibians of Eastern and Central North America. Houghton Mifflin Harcourt Publishing Company, USA.

Pritchard, J. K., M. Stephens, and P. Donnelly. 2000. Inference of population structure using multilocus genotype data. Genetics 155:945–59.

Provan, J., and K. D. Bennett. 2008. Phylogeographic insights into cryptic glacial refugia. Trends in Ecology and Evolution 23:564–571. doi: 10.1016/j.tree.2008.06.010.

Pyron, R. A., and F. T. Burbrink. 2009a. Molecular phylogenetics and evolution neogene diversification and taxonomic stability in the snake tribe Lampropeltini (Serpentes: Colubridae). Molecular Phylogenetics and Evolution 52:524–529. doi: 10.1016/j.ympev.2009.02.008.

———, and ———. 2009b. Systematics of the common kingsnake (*Lampropeltis getula;* Serpentes: Colubridae) and the burden of heritage in taxonomy. Zootaxa 2241:22–32.

Rambaut, A. J., and A. Drummond. 2007. Tracer v1.6. Available from: http://beast.bio.ed.ac.uk/Tracer.

Riddle, B. R. 2016. Comparative phylogeography clarifies the complexity and problems of continental distribution that drove A. R. Wallace to favor islands. Proceedings of the National Academy of Sciences of the United States of America 113:7970–7977. doi: 10.1073/pnas.1601072113.

Rissler, L. J. 2016. Union of phylogeography and landscape genetics. Proceedings of the National Academy of Sciences of the United States of America 113:8079–8086. doi: 10.1073/pnas.1601073113.

Rodriguez, D., M. R. J. Forstner, D. L. McBride, L. D. Densmore, and J. R. Dixon. 2012. Low genetic diversity and evidence of population structure among subspecies of *Nerodia harteri*, a threatened water snake endemic to Texas. Conservation Genetics 13:977–986. doi: 10.1007/s10592-012-0346-x.

Ronquist, F., and J. P. Huelsenbeck. 2003. MRBAYES 3: Bayesian phylogenetic inference under mixed models. Bioinformatics 19:1572–1574.

Ronquist, F., M. Teslenko, P. van der Mark, D. L. Ayres, A. Darling, S. Höhna, B. Larget, L. Liu, M. A. Suchard, and J. P. Huelsenbeck. 2012. MrBayes 3.2: efficient Bayesian phylogenetic inference and model choice across a large model space. Systematic Biology 61:539–542. doi: 10.1093/sysbio/sys029.

Row, J. R., R. J. Brooks, C. A. MacKinnon, A. Lawson, B. I. Crother, M. White, and S. C. Lougheed. 2011. Approximate Bayesian computation reveals factors that influence genetic diversity and population structure of foxsnakes. Journal of Evolutionary Biology 24:2364–2377. doi: 10.1111/j.1420-9101.2011.02362.x.

Ruane, S., R. W. Bryson, R. A. Pyron, and F. T. Burbrink. 2014. Coalescent species delimitation in Milksnakes (Genus *Lampropeltis*) and impacts

on phylogenetic comparative analyses. Systematic Biology 63:231–250. doi: 10.1093/sysbio/syt099.

Seal, J. N., L. Brown, C. Ontiveros, J. Thiebaud, and U. G. Mueller. 2015. Gone to Texas: phylogeography of two *Trachymyrmex* (Hymenoptera: Formicidae) species along the southeastern coastal plain of North America. Biological Journal of the Linnean Society 114:689–698. doi: 10.1111/bij.12426.

Stamatakis, A. 2007. RAxML-VI-HPC: maximum likelihood-based phylogenetic analyses with thousands of taxa and mixed models. Bioinformatics 22:2688–2690.

Stephens, M., and P. Scheet. 2005. Accounting for decay of linkage disequilibrium in haplotype inference and missing-data imputation. American Journal of Human Genetics 76:449–462. doi: 10.1086/428594.

Stephens, M., N. J. Smith, and P. Donnelly. 2001. A new statistical method for haplotype reconstruction from population data. American Journal of Human Genetics 68:978–989. doi: 10.1086/319501.

Swenson, N. G., and D. J. Howard. 2005. Clustering of contact zone, hybrid zones, and phylogeographic breaks in North America. The American Naturalist 166:581–591.

Thomson, R. C., P. Q. Spinks, and H. B. Shaffer. 2018. Molecular phylogeny annd divergence of the map turtles (Emydidae: *Graptemys*). Molecular Phylogenetics and Evolution 121:61–70. doi: 10.1016/j.mpev.2017.11.012.

Townsend, T. M., R. E. Alegre, S. T. Kelley, J. J. Wiens, and T. W. Reeder. 2008. Rapid development of multiple nuclear loci for phylogenetic analysis using genomic resources: an example from squamate reptiles. Molecular Phylogenetics and Evolution 47:129–142. doi: 10.1016/j.ympev.2008.01.008.

Tucker, S. T., R. E. Otto, R. M. Joeckel, and M. R. Voorhies. 2014. The geology and paleontology of Ashfall Fossil Beds, a late Miocene (Clarendonian) mass-death assemblage, Antelope County and adjacent Knox County, Nebraska, USA. GSA Field Guides 36:1–22.

Walker, D., P. E. Moler, K. A. Buhlmann, and J. C. Avise. 1998a. Phylogeographic uniformity in mitochondrial DNA of the snapping turtle (*Chelydra serpentina*). Animal Conservation 1:55–60.

———, ———, ———, and ———. 1998b. Phylogeographic patterns in *Kinosternon subrubrum* and *K . baurii* based on mitochondrial DNA restriction analyses. Herpetologica 54:174–184.

Walley, H. D., and M. V. Plummer. 2000. *Opheodrys aestivus*. Catalogue of American Amphibians and Reptiles 718:1–14.

Waltari, E., R. J. Hijmans, A. T. Peterson, Á. S. Nyári, S. L. Perkins, and R. P. Guralnick. 2007. Locating Pleistocene refugia: comparing phylogeographic and ecological niche model predictions. PLoS One:e563. doi: 10.1371/journal.pone.0000563.

Webb, R. G. 1980. *Thamnophis cyrtopsis* (Kennicott): black-necked garter snake. Catalogue of American Amphibians and Reptiles 245:1–4.

Weinell, J. L., and C. C. Austin. 2017. Refugia and speciation in North American Scarlet Snakes (*Cemophora*). Journal of Herpetology 51: 161–171. doi: 10.1670/15-125.

Accepted: 25 April 2021.
Published online: day Month year.

Supplementary Data

Supplementary data associated with this article can be found online at http://dx.doi.org/10.1670/20-040.S1.

APPENDIX.—Collection localities and GenBank accession numbers for samples included in this study. Samples in bold indicate inclusion in both Sanger and ddRADseq datasets. Str. Label indicates code used to label structure plots, with samples organized from northeast to southwest within each clade. Collection codes abbreviated as follows: CAS: California Academy of Science, FTB: Frank T. Burbrink, KU: University of Kansas Biodiversity Institute and Natural History Museum, LSUMZ: Louisiana State University Museum of Natural Sciences, MVZ: Museum of Vertebrate Zoology, NCSM: North Carolina Museum of Natural Sciences, SR: Sara Ruane, UF: University of Florida Museum of Natural History, UTEP: University of Texas at El Paso Biodiersity Collections, YPM: Yale Peabody Museum of Natural History.

							GenBank accession number			
Catalog number	Species	Clade	Str. label	Locality	Latitude	Longitude	CytB	LAT	NT3	PRLR
FTB1422	***Opheodrys aestivus***	**Main**	24	**AL: Cleburne Co.**	**33.86131**	**−85.52285**				
CAS173661	***Opheodrys aestivus***	**Florida**	43	**FL: Citrus Co.**	**28.88010**	**−82.42718**				
FTB2014	*Opheodrys aestivus*	Main	20	FL: Columbia Co.	30.50995	−82.70642				
FTB2543	*Opheodrys aestivus*	Main	21	FL: Hamilton Co.	30.49706	−82.79439				
UF152372	*Opheodrys aestivus*	Florida	44	FL: Hendry Co.	26.42851	−81.17352				
FTB1733	*Opheodrys aestivus*	Main	25	FL: Holmes Co.	30.94091	−85.80859				
UF170002	*Opheodrys aestivus*	Florida	45	FL: Monroe Co.	25.25649	−80.31342				
FTB2524	***Opheodrys aestivus***	**Main**	16	**FL: Putnam Co.**	**29.73208**	**−81.89759**				
UF175417	*Opheodrys aestivus*	Main	19	FL: Putnam Co.	29.62505	−81.98686				
FTB1748	*Opheodrys aestivus*	Main	18	GA: Brantley Co.	31.26400	−81.96266				
FTB1749	*Opheodrys aestivus*	Main	17	GA: Charlton Co.	30.97194	−81.96015				
FTB1417	*Opheodrys aestivus*	Main	23	GA: Walker Co.	34.60540	−85.08134				
FTB1497	*Opheodrys aestivus*	Main	27	IL: Jackson Co.	37.68668	−89.32342				
FTB1502	***Opheodrys aestivus***	**Main**	26	**IL: Pope Co.**	**37.52703**	**−88.65661**		**–**		
KU331904	***Opheodrys aestivus***	**Main**	38	**KS: Johnson Co.**	**38.57124**	**−94.58430**		**–**		
LSUMZ H3328	*Opheodrys aestivus*	Main	36	LA: Cameron Par.	29.78810	−93.24550				
LSUMZ H3174	*Opheodrys aestivus*	Main	31	LA: East Baton Rouge Par.	30.34331	−91.14430		–		
LSUMZ H18834	*Opheodrys aestivus*	Main	35	LA: Natchitoches Co.	31.43273	−92.94362				
LSUMZ H18369	***Opheodrys aestivus***	**Main**	33	**LA: Ouachita Co.**	**32.29071**	**−92.27465**		**–**		
LSUMZ H15950	*Opheodrys aestivus*	Main	34	LA: Rapides Co.	31.41040	−92.48411				
LSUMZ H20418	*Opheodrys aestivus*	Main	32	LA: Saint Martin Par.	30.37150	−91.63730				
LSUMZ H20453	*Opheodrys aestivus*	Main	28	LA: Saint Tammany Par.	30.55649	−90.01189				
LSUMZ H20640	*Opheodrys aestivus*	Main	29	LA: Washington Par.	30.76580	−90.16090				
MVZ233348	*Opheodrys aestivus*	Main	30	MO: Saint Louis Co.	38.52593	−90.56173				–
FTB430	*Opheodrys aestivus*	Main		MS: Warren Co.	32.25705	−90.76505		–		
MVZ162368	*Opheodrys aestivus*	Main	5	NC: Brunswick Co.	33.92500	−78.30430				
NCSM80128	*Opheodrys aestivus*	Main	6	NC: Brunswick Co.	34.14880	−78.33600		–		
SR388	***Opheodrys aestivus***	**Main**	12	**NC: Hoke Co.**	**35.04512**	**−79.45452**				
NCSM76273	***Opheodrys aestivus***	**Main**	13	**NC: Montgomery Co.**	**35.16280**	**−79.63260**				
NCSM91214	***Opheodrys aestivus***	**Main**	11	**NC: Orange Co.**	**36.07455**	**−79.10090**				
MVZ175965	*Opheodrys aestivus*	Main	8	NC: Wake Co.	35.69570	−78.71450				
MVZ175966	*Opheodrys aestivus*	Main	9	NC: Wake Co.	35.69570	−78.71450				–
NCSM78968	*Opheodrys aestivus*	Main	3	NC: Washington Co.	35.85100	−76.56390				
NCSM82571	*Opheodrys aestivus*	Main	15	NC: Wilkes Co.	36.36000	−80.97840				
SR661	***Opheodrys aestivus***	**Main**	1	**NJ: Burlington Co.**	**39.84422**	**−74.70769**				
SR239	***Opheodrys aestivus***	**Main**	2	**NJ: Cape May Co.**	**39.27456**	**−74.75661**				
YPM18491	*Opheodrys aestivus*	Main	37	OK: Le Flore Co.	34.69130	−94.54220		–		
NCSM79267	*Opheodrys aestivus*	Main	14	SC: Dorchester Co.	33.09510	−80.47900				
FTB2388	***Opheodrys aestivus***	**Main**	22	**TN: Blount Co.**	**35.54188**	**−84.08220**		**–**		
FTB2181	*Opheodrys aestivus*	Texas	41	TX: Coryell Co.	31.41685	−97.55341				
UTEP20508	*Opheodrys aestivus*	Main	39	TX: Morris Co.	32.91332	−94.73537				
UTEP19733	*Opheodrys aestivus*	Texas		TX: Sutton Co.	30.57427	−100.82482		–	–	–
MVZ150192	***Opheodrys aestivus***	**Texas**	42	**TX: Travis Co.**	**30.26700**	**−97.74300**				
FTB2163	*Opheodrys aestivus*	Main	40	TX: Trinity Co.	31.13580	−94.94225				
FTB1227	*Opheodrys aestivus*	Main	4	VA: Chesterfield Co.	37.29660	−77.60143				
FTB2651	*Opheodrys aestivus*	Main	10	VA: Halifax Co.	36.83234	−78.78107				
FTB1222	*Opheodrys aestivus*	Main	7	VA: Prince Edward Co.	37.20247	−78.33847				
YPM20788	*Opheodrys vernalis*	Vernalis East	46	CT: Windham Co.	41.94897	−72.10521				–
YPM13102	***Opheodrys vernalis***	**Vernalis East**	**47**	**ME: Somerset Co.**	**45.30798**	**−69.91898**				
UTEP18721	*Opheodrys vernalis*	Vernalis West	48	NM: Lincoln Co.	33.38014	−105.62846				
UTEP19513	*Opheodrys vernalis*	Vernalis West	49	NM: Lincoln Co.	33.46625	−105.78868				
SR705	*Cemophora coccinea*	Outgroup		NJ: Cumberland Co.	39.34464	−74.97247				
SR315	*Lampropeltis getula*	Outgroup		NJ: Ocean Co.	39.95130	−74.47190				
SR278	*Pantherophis guttatus*	Outgroup		NJ: Burlington Co.	39.80001	−74.55049				
SR248	*Pituophis melanoleucus*	Outgroup		NJ: Atlantic Co.	39.55648	−74.74002				
SR216	*Nerodia sipedon*	Outgroup		NJ: Burlington Co.	39.95544	−74.61765		–		

Queries for hpet-55-04-05

This article has been edited and typeset from the submitted materials. Please check proofs carefully for accuracy and follow the Allen Press Guide to PDF Annotation when marking revisions. Do not edit the PDF directly.

If present, queries will be listed below with corresponding numbers in the margins or may appear as PDF comments addressed to the author or editor. If a correction is desired in response to a query, mark the necessary changes directly in the proof using the appropriate annotation tool. If no change is desired, please highlight the query number in the margins and mark "No change needed" or reply to the PDF annotation with "No change needed".

1. **Author: there is a sentence fragment after figure 5 caption referring to Appendix. Please remove or fix. Thanks. Copy editor**